Experimental investigation on performance parameters affecting the efficiency of water type PV/Thermal collectors with modified absorber configurations

Sıvı akışkan tipli PV/Termal kolektörlerin verimliliğini etkileyen performans parametrelerinin farklı tasarlanmış soğurucular ile deneysel incelenmesi

Yazar(lar) (Author(s)): Halil İbrahim DAĞ[1], Günnur KOÇAR[2]

ORCID[1]: 0000-0001-9346-8451

ORCID[2]: 0000-0003-1142-8574

Experimental Investigation on performance Parameters Affecting the Efficiency of Water Type PV/Thermal Collectors with Modified Absorber Configurations

Highlights

- ❖ *Thermal and electrical efficiency of water-type photovoltaic/thermal (PV/T) modules were investigated./ Su tipli fotovoltaik/termal (PV/T) kolektörlerin termal ve elektriksel verimlilikleri incelenmiştir.*

- ❖ *5 PV/T modules differed in thermal structure with different diameters, amount and layout of absorber tubes, and type of absorber sheets were fabricated./ Farklı çaplar, miktar ve dizilimlere sahip soğurucu borular ve soğurucu levhalar kullanılarak, laminasyon tekniği ile, beş adet PV/T kolektör üretilmiştir.*

- ❖ *The electrical efficiency of all samples under Standard Test Conditions was tested by a solar simulator./Bir güneş simülatörü kullanılarak tüm numunelerin elektriksel verimliliği Standart Test Koşullarında test edilmiştir.*

- ❖ *Outdoor tests were carried out to investigate the effect of temperature on PV modules in ambient conditions./ PV/T numuneleri kullanılarak, dış ortam koşullarında ısıl enerjinin PV modüllere olan etkisi incelenmiştir.*

- ❖ *In order to determine the efficiency of the units, parameters such as solar irradiation, voltage and current values, inlet and outlet water temperature and flow rate of PV/T modules and ambient temperature were measured./ Numunelerin verimliliklerini tespit için; güneş ışınımı, voltaj ve akım değerleri, PV-T modüllerdeki su giriş, çıkış sıcaklıkları, suyun debisi ve dış ortam sıcaklığı gibi değerler ölçümlenmiştir.*

Graphical Abstract
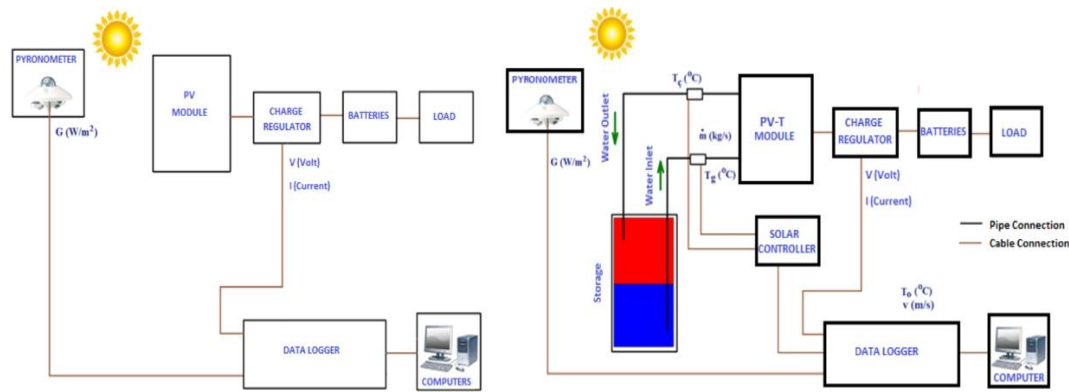
Figure. Block diagram of the experimental set-up established for a) PV B) PV/T tests and measured parameters.

Aim

The aim of the study is to modify the thermal collectors and optimally combine with PV collectors to improve their efficiency and performance and to reduce the heat-induced efficiency loss of photovoltaic (PV) modules and to ensure maximum energy conversion (combined electrical and thermal).

Design & Methodology

By using identical photovoltaic (PV) cells, one PV module and five PV/T modules differed in thermal structure with different diameters, amount and layout of absorber tubes, and type of absorber sheets were fabricated with lamination technique.

Originality

The novelty aspect of this study is that it is the first study that compares PV/T modules with five different thermal configurations and that the lamination technique was used for the first time to join the thermal part to the PV module for the PV/T module fabrication.

Findings

Total efficiency value of PV/T modules in outdoor conditions were attained between 60.68% and 67.14%.

Conclusion

Compared to the other modules, the thermal part of the PVT-3 module provides more efficient cooling in terms of cell temperature values, enabling cells in this module to convert energy at lower cell temperatures.

Declaration of Ethical Standards

The author(s) of this article declare that the materials and methods used in this study do not require ethical committee permission and/or legal-special permission.

Experimental Investigation on Performance Parameters Affecting the Efficiency of Water Type PV/Thermal Collectors with Modified Absorber Configurations

Halil İbrahim DAĞ[1*], Günnur KOÇAR[2]

[1]SOLIMPEKS Solar, 42050 Konya, Turkey
[2]Ege University, Solar Energy Institute, 35100 İzmir, Turkey

ABSTRACT

In this study, efficiency of water-type photovoltaic/thermal (PV/T) modules that convert solar energy into both electrical and thermal energy were investigated. By using identical photovoltaic (PV) cells, one PV module and five PV/T modules differed in thermal structure with different diameters, amount and layout of absorber tubes, and type of absorber sheets were fabricated with lamination technique. Firstly, the electrical efficiency of all samples under Standard Test Conditions was tested by a solar simulator. Efficiency values were between 12.56% and 12.68% under STC. Furthermore, outdoor tests were carried out to investigate the effect of temperature on PV modules in ambient conditions using PV/T samples. In order to determine the efficiency of the units, parameters such as solar irradiation, voltage and current values, inlet and outlet water temperature and flow rate of PV/T modules and ambient temperature were measured. It was observed that the electrical performance of PV/T modules was higher than that of the PV module due to the cooling effect of water circulation over the cells. PV/T module with the highest thermal efficiency was also determined. Total efficiency value of PV/T modules in outdoor conditions were attained between 60.68% and 67.14%.

Keywords: PV, solar thermal, PV/T, performance characteristics, experimental study.

Sıvı Akışkan Tipli PV/Termal Kolektörlerin Verimliliğini Etkileyen Performans Parametrelerinin Farklı Tasarlanmış Soğurucular ile Deneysel İncelenmesi

ÖZ

Bu çalışmada; güneş enerjisini hem elektrik enerjisine hem ısıl enerjiye dönüştüren, su tipli fotovoltaik/termal (PV/T) kollektörlerin verimlilikleri incelenmiştir. Özdeş fotovoltaik (PV) hücreler kullanılarak; bir adet PV modül ve farklı çaplar, miktar ve dizilimlere sahip soğurucu borular ve soğurucu levhalar kullanılarak, laminasyon tekniği ile, beş adet PV/T kollektör üretilmiştir. Öncelikle; Standard Test Koşulları'nda bir güneş simülatörü ile tüm numunelerin elektriksel verimliliği test edilmiştir. STK'da verimlilik değerleri %12,56 ile %12,68 olarak ölçülmüştür. Sonrasında; PV/T numuneleri kullanılarak, dış ortam koşullarında ısıl enerjinin PV modüllere olan etkisi incelenmiştir. Numunelerin verimliliklerini tespit için; güneş ışınımı, voltaj ve akım değerleri, PV-T modüllerdeki su giriş, çıkış sıcaklıkları, suyun debisi ve dış ortam sıcaklığı gibi değerler ölçümlenmiştir. Su devir daiminin hücrelerin soğumasına etkisinden kaynaklı, PV/T kollektörlerdeki elektriksel verimin PV modüldekinden fazla olduğu gözlemlenmiştir. PV/T kollektörler arasında en yüksek ısıl verimliliğe sahip örnek de tespit edilmiştir. PV/T kollektörlerin, dış ortam koşullarındaki toplam verimliliklerinin %60,68 ile %67,14 arasında olduğu görülmüştür.

Anahtar kelimeler: PV, güneş termal, PV/T, performans parametreleri, deneysel çalışma.

1.INTRODUCTION

The rapid population growth and industrialization of the present day cause a sudden increase in the demand for energy, a key indicator reflecting the economic and social development potential of countries. It is acknowledged that there is a linear relationship between energy consumption and social development and that energy consumption increases with economic development and increase in welfare. As a foundation of prosperity and progress of nations, fossil fuel based energy sources are expected to be exhausted in the short term, renewable energy sources, on the other hand, represent the sustainable potential that is not fully utilised. Solar energy is, among others, a renewable and sustainablesource with a vast potential that is never fully exploited [1]. Electrical energy is generated by using photovoltaic (PV) solar cells. Photovoltaic solar cells are

---

*Sorumlu Yazar (Corresponding Author)
e-posta : halil.dag@solimpeks.com

semiconductor devices that convert solar energy into electrical energy. In a period of intense change in climate, environmentally friendly photovoltaic solar cells have become the future hope of humanity as they can directly convert the energy of the sun, which is an endless source of energy, into electrical energy, in harmony with nature's millions of years of balance [2].

The history of solar cells dates back to the 19th century. In 1839, Alexandre Edmond Becquerel discovered the first photovoltaic effect in his experiments with platinum plates. The first silicon solar cell was developed in 1954 at Bell Laboratories by two scientists named Pearson and Fuller. Next, silicon-based solar cells were first used by the USA in a spacecraft called Vanguard-I [3].

Today, huge decrease in costs due to developments in solar cell technology in recent years has rendered this technology more affordable and available, and eliminated the need for huge amounts of government support. Thus, solar cell installations have now become feasible. A latest report estimates that the global cumulative PV capacity increased exponentially especially after 2010 and will reach above 700 GW by the end of 2020 [4].

As a main drawback, the efficiency of PV solar cells decreases with increasing temperature. Every 1°C increase in PV solar cells results in a loss of efficiency between 0.45 and 0.50% in electricity generation [5]. In order to reduce this temperature effect, studies have been carried out comprising both the PV module and thermal part. The first study was conducted by KW Boer who developed an air-type PV/T module at the University of Delaware in 1973 [6]. Later, in 1976, a water-type PV/T study was performed by Martin Wolf [7]. After these pioneering studies, great quanta of studies on PV/T applications have increasingly been performed [8-11].

To name a few, Rejeb et al. (2015) published a comprehensive study on numerical modelling of PV/T systems. They investigated the performance of PV/T collectors under semi-arid climatic conditions. In numerical modelling, six basic components of the PV/T system were considered including glass cover, PV module, the absorber plate, pipe, fluid in the pipe, and insulation. Their study yielded results that were highly consistent with experimental data and it was seen that the thermal and electrical efficiency of a PV varied significantly according to the water input temperature, the number of glass covers, and the thermal conductivity coefficient between the PV and the absorber plate [12]. Liang et al. (2015) examined the performance of a PV/T system developed by filling the conventional PV/T solar collector with graphite. They measured the electrical efficiency of the graphite-filled PV/T and conventional PV/T between 08:00 and 16:00 as 6.46% and 5.15%, respectively. They found the highest efficiency of the graphite filled PV/T system as 7.2% and determined the highest Primary Energy Saving efficiency as 48% at 10:35. They also noted that electrical efficiency can be

increased by lowering the temperature of the back layer and thermal efficiency can be increased by lower input temperature [13]. Aste et al. (2019) designed PV/T systems with an innovative glass structure and emphasized the mathematical model of this system. They used thin-film PV technology in the PV/T system and coated it with the roll-bond flat absorber. They compared the daily and annual measurements of the system with those of a standard PV module. While they observed 13.4% efficiency in standard PV systems, they reported a total increase of 42%, including 13.2% electrical efficiency and 28.8% thermal efficiency, in the designed PV/T systems [14].

In this study, modified thermal collectors that produce thermal energy from solar energy and photovoltaic modules have been optimally combined and their efficiency and performance measurements have been performed to reduce the heat-induced efficiency loss of photovoltaic (PV) modules and to ensure maximum energy conversion (combined electrical and thermal). The novelty aspect of this study is that it is the first study that compares PV/T modules with five different thermal configurations and that the lamination technique was used for the first time to join the thermal part to the PV module for the PV/T module fabrication.

2. MATERIAL AND METHOD

2.1. Description of the Flat-Plate solar Collectors and manufacturing method

Solar energy is most commonly utilised through flat-plate collectors. The schematic of a typical flat-plate solar collector is shown in Fig 1. Flat-plate solar collectors are economical, environmentally friendly, practical, and simple heat exchangers used in low temperature loads and simple thermal applications. No complex technology is required for their production. Flat-plate solar collectors are used for many purposes such as domestic hot water and heating systems, cooling systems, drying of agricultural products, heating swimming pools, and heating greenhouses. In flat-plate solar collectors, the conversion of solar energy to heat energy takes place by the absorption of solar radiation on black or special coated surfaces and transferring the heat from the surface with increasing temperature to a fluid. Although these collectors are divided into two main groups as water and air type, this study focuses on the efficiency of water type flat-plate solar collectors, information only about these collectors is given.

In a flat-plate solar collector, the cold fluid (water) is distributed from the manifold pipe to the absorber pipes which are placed in the length of the collector and which are in contact with the absorber plate. The temperature of the absorber plate increases as it absorbs the solar radiation falling on it. Heat is then transferred from the absorber plate to the fluid by conduction and convection. The heated fluid is collected in the collector pipe and transferred for utilisation. In this research, photovoltaic collector and thermal absorber is combined.
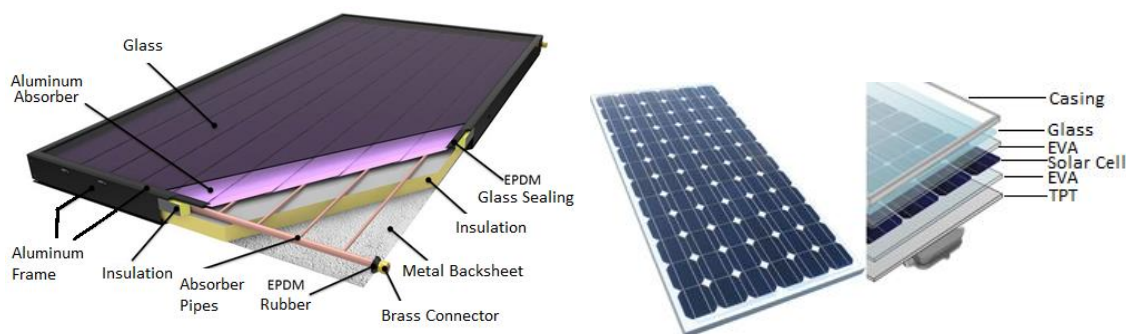
Fig 1. Schematic view of a flat-plate solar collector and a PV unit

Table 1. Properties of the PV cell used in the preparation of the samples

Manufacturer	:	SF-PV Shunfeng Photovoltaic Int. Ltd.
Type	:	Single crystal silicon (Si)
Dimensions	:	125 mm x 125 mm
Thickness	:	200±20 μm
Average cell efficiency	:	15.40%

The properties of the PV cells used in the modules are presented in Table 1. To manufacture the PV/T collectors and a PV unit, the assembly of PV cells was performed in a stringer (cell assembly) machine (2BG S.R.L, Model: TS600PLUS). The PV cells are placed in the chambers. 12 PV cells are automatically soldered to be connected in series with silver solder wires (ribbons). Next, with the help of a robotic arm (KPC-ed05), groups of 12 cells from the stringer machine are placed on the glass at desired intervals to form 6 series connections. Each series of 12 cells (72 PV cells in total) is manually reassembled in series. In addition, after the soldering process, EVA (Ethyl Vinyl Acetate) is placed on the cells and TPT (Tedlar Polyester Tedlar) is placed on the EVA. EVA and TPT layers have the thermal conductivity of 0.23 W/m.K and 0.36 W/m.K, respectively. Thus, the structure is made ready for lamination. Finally, the resulting structure is subjected to heat treatment and vacuuming in the lamination machine (2BG S.R.L, Model: L640A), and the PV cells are laminated to glass and TPT. Thus, the desired PV module is made ready.

The manifold and absorber pipes that come in a roll are cut to the desired dimensions in the roll opening, pipe straightening, and length cutting machines, for use in the thermal absorber panel. In this study, copper pipes of four different diameters and thicknesses were used. The absorber pipes were 8 and 10 mm in diameter and 0.45 mm in wall thickness; the manifold pipes were 18 and 22 mm in diameter and 0.70 mm in wall thickness. Perforations are performed on the manifold pipes according to the design at the intervals specified in the automatic pipe drilling machine (SUNRISE Model: TUBOCOP 1500). In addition, brass male fittings which were ¾" in diameter were fitted on the two ends of the pipes. The desired number of absorber pipes are welded to the manifold pipes with oxygen welding (SUNRISE Model: SB-FBM-T2). Then, the pressure is tested in the test device (SUNRISE Model: SR-CFL-TESTER) to check for leaks in pipes and welds. Thus, the manifold pipes are made ready to be assembled with the manifold plate. The copper or aluminium absorber plate is cut to the desired size with the roll opening and cutting machine (MEAN WELL Model: DR4524), and made ready for laser welding. After the absorber pipes are placed on the prepared copper or aluminium strip, they are laser welded with the laser welding device (SUNRISE Model: SR-LWL-F2500). Accordingly, the thermal absorber part is completed. Fig 2 illustrates the thermal absorber configurations of the PV/T modules, respectively.
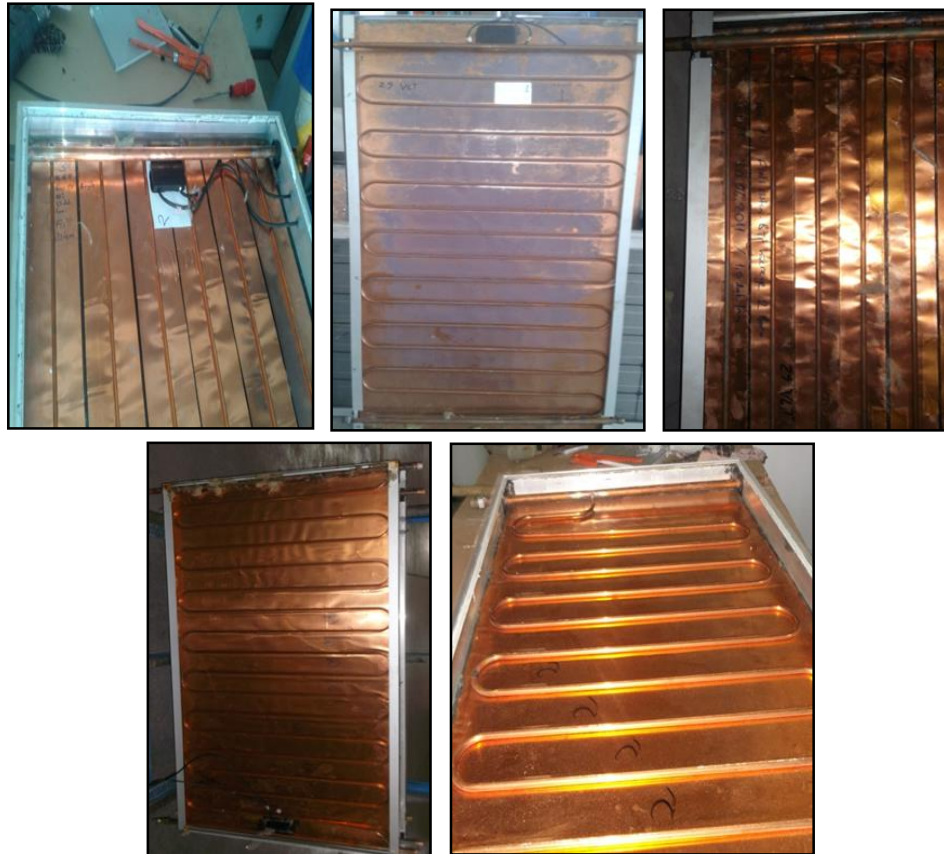
Fig 2. Inner view of the thermal absorbers of PVT-1, PVT-2, PVT-3, PVT-4 and PVT-5

In the last phase of the production, assembly of the PV modules with the thermal part is carried out. EVA is placed between the prepared photovoltaic module and the thermal absorber and the lamination process is carried out in the laminating machine mentioned above. Thus, the assembly of the PV/T is completed. The junction box, where the output conductors of the photovoltaic cells are wired together and which encapsulate bypass diodes and
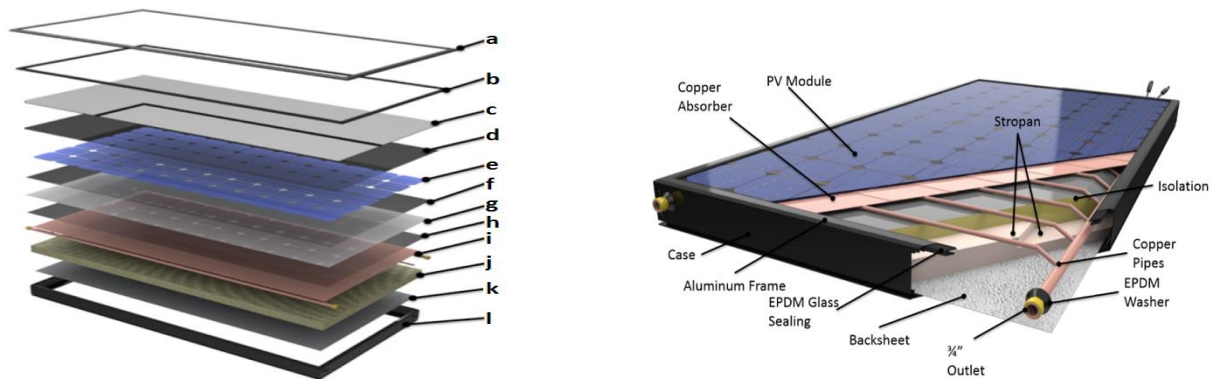
Fig 3. Layered internal structure of the PV/T module

a	Aluminium frame for fixing the glass to the aluminium enclosure.	**g**	Black Tedlar Polyester Tedlar (TPT), back layer against cell breakage.
b	EPDM (Ethylene Propylene Rubber) wrapped for water impermeability.	**h**	EVA for laminating the copper strips in the thermal absorber to the TPT.
c	Low-iron Glass with high radiation permeability on the front	**i**	Thermal Absorber through connecting copper pipes and copper strips
d	Flexible EVA for laminating PV cells to the glass.	**j**	Rock wool for insulation material to reduce heat losses in the PV-T module.
e	Monocrystalline-Si PV cell layer	**k**	Back Sheet is aluminium plate for protective cover for the PV-T
f	Flexible EVA for laminating PV cells to the TPT.	**l**	Aluminium frame to protect the PV-T module

the output (+) and (-) cables, are placed on the back side of the absorber plate. For the insulation, firstly, the stone wool and sidewalls for heat insulation are placed in the aluminium enclosure with corners connected with rivets and a base sheet attached. After the EPDM wick was laid on the laminated PV panel and the absorber glass, they are placed in the aluminium enclosure. The PV/T module is ready for installation. The internal structure and parts and the cross-sectional view of the PV/T modules are presented in Fig 3.

The PV/T configurations investigated in this study were manufactured through the same steps by using identical PV cells. The PV/T modules are diversified in terms of pipe diameters, number of pipes, and type of absorber plate. The main aim of this study is to examine the PV/T modules produced under the same conditions but with materials of different diameters and types and to determine the optimum PV/T module. To this end, five different types of PV/T modules with materials with different properties were prepared. Furthermore, to compare the efficiencies of the PV/T modules with the efficiency of a PV module, a PV module was also prepared. The specifications of the prepared PV/T modules and PV module are given in the Table 2.

burst pipes, water leakage or swelling were detected in any of the modules. For STC, a solar radiation spectrum of 1000 W/m² (AM 1.5) and a temperature of 25°C are defined as standard test conditions solar cells or modules. A solar simulator with Xenon lamps and suitable filters are used to perform such tests in a very short time and without heating the PV module. In order to determine the electrical efficiencies of 5 PV/T modules and 1 PV module, I-V measurements in STC were performed with the solar simulator (QUICKSUN Model: 540LA). The solar simulator has current and voltage measurement accuracy of ±0.2% and monitoring cell and ambient temperature with precision IC sensors with 0.1°C resolution and ±1°C accuracy.

For outdoor tests, The PV modules and water-type PV/T modules were installed at an angle of 30^0 degrees on the south-facing at the backyard of Institute of Solar Energy in Ege University using appropriate mounting kits. The thermal system connections of the PV/T modules (tank, pump, piping, etc.) were achieved and the system was operated with water pressure of 2.5 bar. A pyranometer (Kipp and Zonen with sensitivity of 17.99 × 10−6 V/W/m²) was placed at the same angle as the PV module and PV/T modules to prevent it from being shadowed or

Table 2. Thermal absorber specifications of the PV/T modules

Module	Absorber Pipe Diameter	Manifold Pipe Diameter	# of Absorber Pipes	Type of Absorber Plate
PV/T 1	Φ8 mm	Φ22 mm	6	Finned plate
PV/T 2	Φ10 mm	Φ18 mm	16	Serpentine
PV/T 3	Φ8 mm	Φ22 mm	12	Finned plate
PV/T 4	Φ10 mm	Φ22 mm	16	Serpentine
PV/T 5	Φ10 mm	Φ22 mm	13	Serpentine

2.2. Test procedure

The produced PV/T modules were first tested with water with a pressure of 25 bar with the Pressure Tester (SUNRISE Model: SR-CFL-TESTER). The pressure tester has accurate pressure control and measurement ranging from 2 bars to 70 bars with accuracy pressurization of 1%. Following the pressure testing process, all modules were examined inspected and no

casting a shadow over the panels. The wiring work and connection of electrical equipment were performed in the PV/T modules. K type thermocouples were placed on the PV/T modules and connected to the controller. Finally, to obtain data from data loggers (DT500), 2 computers were placed in the building, connections were made with the computers and data were stored. Fig 4 shows the experimental procedures of the PV and PV/T modules.
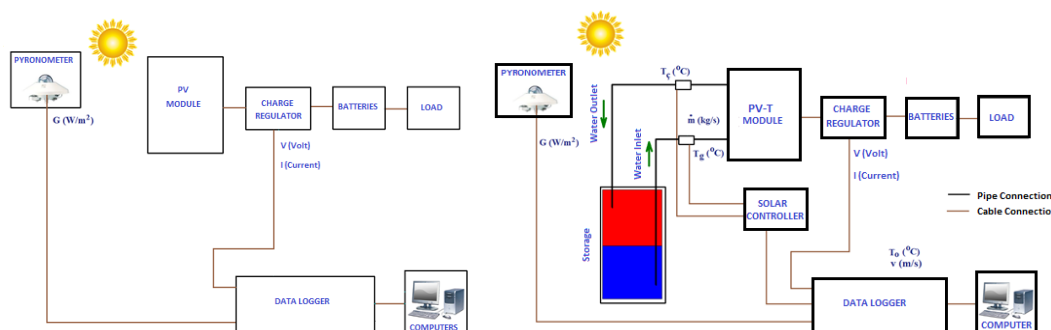
Fig 4. Block diagram of the experimental set-up established for a) PV B) PV/T tests and measured parameters.
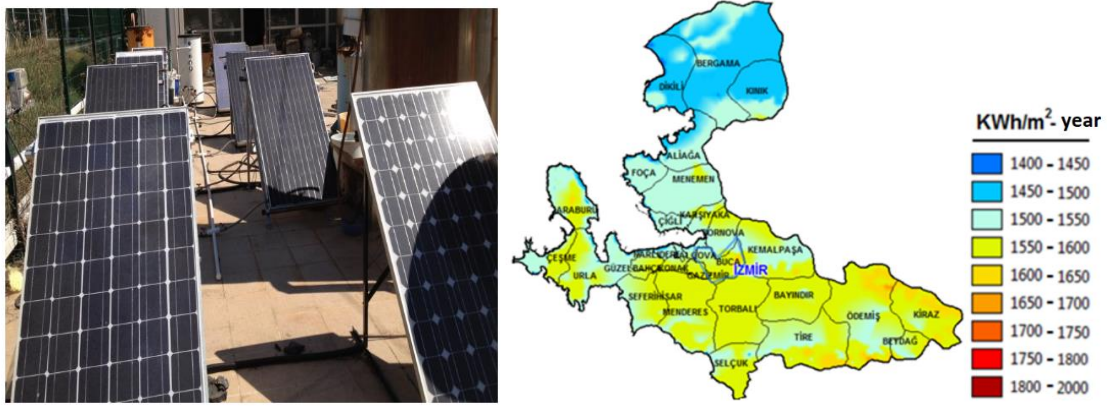
Fig 5. View of the experimental setups at Institute of Solar Energy in Ege University and solar map of Izmir

The study aims to determine the thermal and electrical efficiencies of the PV/T modules experimentally and compare the results. The experiments were performed between April and September 2012. The measurements were achieved between sunrise and sunset. Current, voltage, ambient temperature, input and output water temperature, and solar radiation values were measured.

Izmir is geographically located in the west coast of Turkey within the Aegean region, with latitude and longitude of 38°24'45.83"N, 27°8'18.17"E and elevation from sea level is 30 m. The city has Mediterranean climate with relatively mild winters, hot and sunny summers. Fig 5 shows the view of the experimental site and solar potential of the city which is around 1550-1600 kWh/m^2-year.

3. MATHEMATICAL MODELLING

3.1. Electrical Characteristics of a Photovoltaic Module

In an ideal pn junction, the total current is the sum of the electron and hole currents that are constant along the depletion layer. The total current in the pn junction is shown as [15]

$$I = I_s \left[\exp\left(\frac{eV}{kT}\right) - 1 \right]$$
(1)

Where V denotes the voltage value applied in the reverse or forward feed, I_s is the reverse-saturation current, e is electron charge (1.6x10^{-19} C), k is Boltzmann constant (1.38x10^{-23} J/K), and T is absolute temperature, respectively.

The equivalent circuit of a solar cell consists of a parallel connection of a diode electronically representing a pn junction and a current source representing the photocurrent generation by the light. The net current of the circuit is equal to the difference between the diode current and the photocurrent

$$I = I_s \left(\exp\frac{eV}{nkT} - 1 \right) - I_L$$
(2)

Here, n represents the ideality factor and I_L represents the photocurrent generated by the excess carriers as a result of solar radiation *(light generated)* [16].

Important parameters for solar cell short circuit current are Isc, and open circuit voltage, Voc. The short-circuit current is the current that occurs when there is no resistance on the circuit, i.e., the voltage on the circuit is equal to zero *(V = 0)*. In this case, the short-circuit current is equal to the photocurrent *($Isc = I_L$)*. An open circuit voltage occurs when no current passes through the circuit *(I=0)*. An open circuit voltage is V_{oc} [16],

$$V_{oc} = \frac{kT}{q} ln \left(\frac{I_L}{I_s} + 1 \right) \approx \frac{kT}{q} ln \left(\frac{I_L}{I_s} \right)$$
(3)

The maximum power that can be obtained from a solar cell is the product of the maximum current, I_m and the maximum voltage V_m values of the solar cell under radiation.

One of the important parameters for a solar cell is the, FF, *fill factor* [16]

$$FF = \frac{V_m I_m}{V_{oc} I_{sc}}$$
(4)

Energy conversion efficiency of a solar cell, η_e defines the ratio of the solar energy converted into the electrical energy. Efficiency of a solar cell is calculated as follows [16]

$$\eta_e = \frac{V_m I_m}{P_{in}} = FF \frac{V_{oc} I_{sc}}{P_{in}}$$
(5)

Here, P_{in} is the total radiation power falling on the solar cell.

The IV characteristic of a module is similar to the IV characteristic of one of the solar cells that form it and can be explained by the same equations. The difference here is that the reverse saturation current, diode factor, series, and parallel resistors represent the whole module and they depend on the type, number and electrical connection of the cells. The output current of the PV module composed of N series-connected solar cells is as follows [17];

$$I = I_L - I_s \left\{ exp \left[\frac{V + IR_s}{nNV_T} \right] - 1 \right\} - \frac{V + IR_s}{R_p}$$
(6)

Where I denotes the output current of the module, I_L is photocurrent, N is the number of series-connected solar cells, n is diode ideality factor, R_s is series resistance, R_p is parallel resistance, $V_T = kT/q$ is thermal voltage, T is

the temperature of the solar cell, k is Boltzmann constant $(1.38 \times 10^{-23}$ J/K), q is electric charge $(1.6 \times 10^{-19}$ C), and V is the terminal voltage of the module, respectively.

80 - 90% of the radiation falling on the surface of a module is transferred as heat and therefore the operating temperature of the module can vary within a wide range. Although an increase in the temperature of the module increases the photocurrent, hence the short circuit current (I_{SC}), the open-circuit voltage (V_{OC}) decreases due to electron-phonon scattering caused by the increase of thermal lattice vibrations and the decrease in carrier mobility. A rapid decrease in open-circuit voltage will lead to a decrease in the fill factor value and thus a decrease in the efficiency of the module [18]. The effect of temperature on the I-V characteristics of a PV module is shown in Fig 6. The operating temperature of the module varies depending on the ambient temperature and the penetrating solar radiation and the design and placement of the module. These effects in the design are given by the *Nominal Operating Cell Temperature (NOCT)* of the module.

The efficiency of a module is defined as the ratio of the power obtained from the module to the solar radiation power falling on the module [18].

$$\eta_e = \frac{V_m I_m}{P_{in}} = \frac{V_m I_m}{A_m G} \tag{7}$$
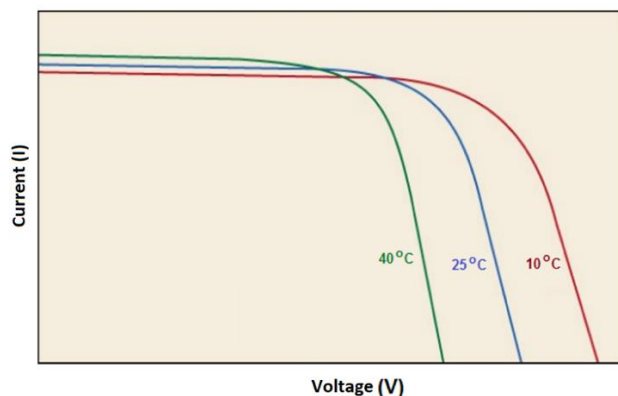
Fig. 6. IV characteristics of the PV module at different temperatures

where V_m *denotes* maximum module output voltage, I_m is the maximum module current, A_m is module nominal area, G is solar radiation values falling on the surface of the module. The fact that the efficiency of a module is dependent on the temperature, is an important parameter in the operation of photovoltaic systems. An instantaneous change in the efficiency of a module depending on the temperature is shown as [18]

$$\eta_e = \eta_{ref} + \mu_{P,mp}\left(T_c - T_{c,ref}\right) \tag{8}$$

η_{ref} is the reference module efficiency defined under standard test conditions, T_c is cell temperature, and $T_{c,ref}$ is the reference temperature (298 K). $\mu_{P,mp}$ represents the way in which the module efficiency decreases linearly depending on temperature for many models and is a

negative number. The $\mu_{P,mp}$ value for silicon is -4.5×10^{-3} K^{-1} [18, 19]. Maximum power point efficiency coefficient is calculated as follows [20]

$$\mu_{P,mp} = \frac{d\eta}{dT} = \left(I_m \frac{dV_m}{dT} + V_m \frac{dI_m}{dT}\right)\frac{1}{A_m G_r} \tag{9}$$

In many models, the temperature-induced short-circuit current variation is relatively small compared to the open-circuit voltage variation; so it is neglected and therefore, the temperature coefficient of the module efficiency depends on the variation of the open-circuit voltage with the temperature. Because of these reasons, $\frac{dV_m}{dT}$ is approximately equal to $\frac{dV_{oc}}{dT}$. The temperature coefficient of the maximum power point efficiency is more simply expressed as follows [17]

$$\mu_{P,mp} = \frac{d\eta}{dT} = \left(I_{mp}\frac{dV_{oc}}{dT}\right)\frac{1}{A_m G} \tag{10}$$

3.2. Thermal Analysis of Flat-Plate Solar Collectors

The collector is evaluated as a control volume and instantaneous energy conservation is applied for the whole collector and the following equation is obtained [21].

$$Q_g = A_t G = Q_f + Q_k + Q_d \tag{11}$$

Here, A_t is surface area of the collector (m^2), G is Instantaneous solar radiation on the collector (W/m^2), Q_g is the solar energy penetrating into the absorber plate (W), Q_f is the useful energy transferred to the fluid (W), Q_d is the stored energy (W) and Q_k is total heat loss (W).

The amount of useful energy (Q_f) transferred from the collector to the fluid can be calculated with the following equation if the water input (T_g) and output temperature ($T_ç$) and flow rate are determined as [21]

$$Q_f = \dot{m}c_p\left(T_ç - T_g\right) \tag{12}$$

The total heat loss coefficient (K) between the absorber plate and the environment is the sum of the heat loss coefficients from the lower surface (K_{down}) and the upper surface (K_{up}) of the collector and is expressed by [21]

$$K = K_{down} + K_{up} \tag{13}$$

Instantaneous collector efficiency is defined as the rate at which the solar radiation falling on the surface is transferred to the fluid as useful energy and is calculated as [21]

$$\eta_t = \frac{Q_f}{Q_g} = \frac{\dot{m}c_p(T_ç - T_g)}{A_t G} \tag{14}$$

Where, G (W/m^2) represents the instantaneous radiation falling on the surface of a collector and A_t is the are of the collector (m^2). The efficiency is evaluated according to the operating point parameter calculated by the following equation. The operating point parameter is calculated by the following equation depending on the fluid input temperature (T_g) and environmental conditions (T_o) [21].

$$P = \frac{t_g - t_a}{G} \quad (15)$$

Heat losses are taken into account, Q_f, [21]

$$Q_f = A_t[S - U_L(T_{p,m} - T_o)] \quad (16)$$

Where, S denotes absorbed solar energy, U_L is heat loss coefficient of the whole collector, $T_{p,m}$ is the average plate temperature, and T_o is ambient temperature. It is further modified as follows [22];

$$Q_f = A_t F_R[S - U_L(T_g - T_o)] \quad (17)$$

where,

$$F_R = \frac{mC_p}{A_t U_L}\left[1 - \exp\left(-\frac{A_t U_L F'}{mC_p}\right)\right] \quad (18)$$

where, F' denotes the collector efficiency factor and is shown as [23];

$$F' = \frac{1/U_L}{W\left[\frac{1}{U_L[D_0+(W-D_0)F]}+\frac{1}{C_b}+\frac{1}{\pi D_i h_{fi}}\right]} \quad (19)$$

Where, C_b denotes the conductivity between the absorber fin and the pipe, h_{fi} is thermal conductivity coefficient of the fluid, and *F* is absorber fin efficiency factor which is calculated as follows [21].

A schematic view of an absorber plate is given in Fig 7 below.
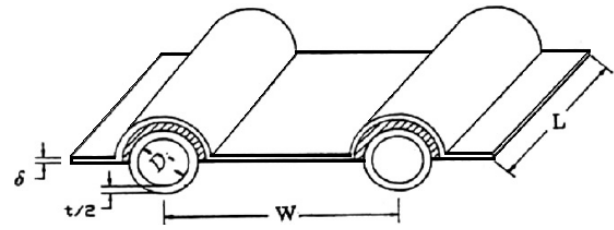
Fig. 7. Schematic view of an absorber plate

4. RESULTS AND DISCUSSION

In the experiments carried out under STC, electrical parameters and efficiencies of five different water-type PV/T modules and an identical PV module were measured. Besides, electrical and thermal analysis of the water-type PV/T modules were performed and the relevant results were obtained. To determine the thermal efficiencies of the modules, surface temperatures, water inlet and outlet temperatures, ambient temperature, solar radiation values, thermal efficiency, thermal gain, and
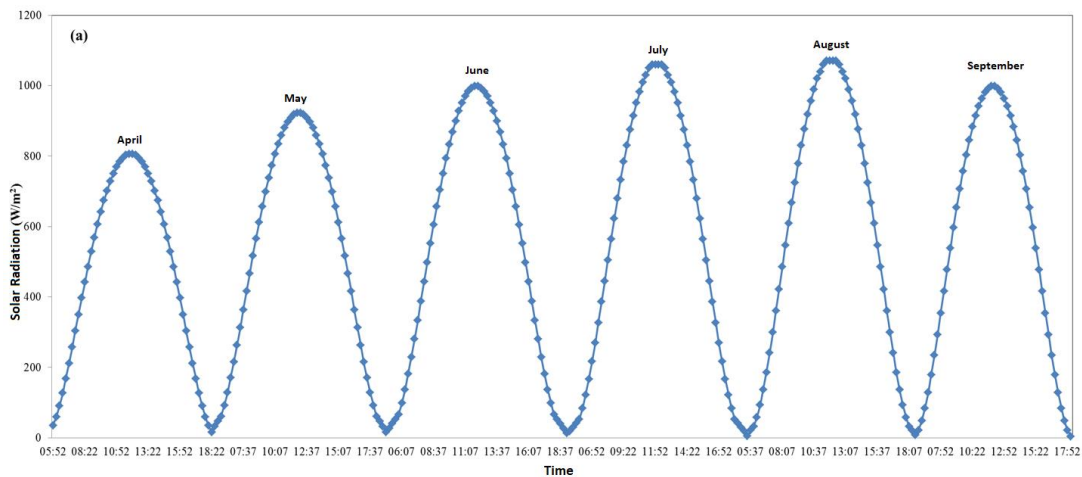
Fig. 8. Average solar radiation values between April and September

$$F = \frac{\tanh(x)}{x} \quad (20)$$

And x is calculated as

$$x = \sqrt{\frac{U_L}{k\delta}}\left(\frac{W-D_0}{2}\right) \quad (21)$$

Where;

$$D_0 = D_i + t \quad (22)$$

Where D_i denotes the diameter of the pipe, *W* is the distance between two pipes, and δ is the thickness of the absorber plate.

Lastly, total efficiency of PV/T modules is defined as the sum of electrical and thermal efficiencies [23, 24] and given as $\quad \eta_T = \eta_t + \eta_e \quad (23)$

flow rates were recorded and analysed. Furthermore, to determine the electrical conversion efficiencies of both PV/T modules and the PV module, their current and voltage values were determined and compared. All these electrical and thermal measurements are used to find out the efficiency improvement by cooling off the PV cells. Then, efficiency rates are compared to determine the optimum absorber structure.

The solar radiation values were measured continuously between April 1, 2012, and September 30, 2012, by means of a pyranometer placed at the same angle as the modules. Data were taken every 15 minutes from sunrise to sunset. Monthly average solar radiation values are presented in Fig 8. As can be seen from the figure that the maximum values of radiation are 806 W/m² for April, 922 W/m² for May, 998 W/m² for June, 1060 W/m² for July, 1070 W /m² for August, and 998 W/m² for
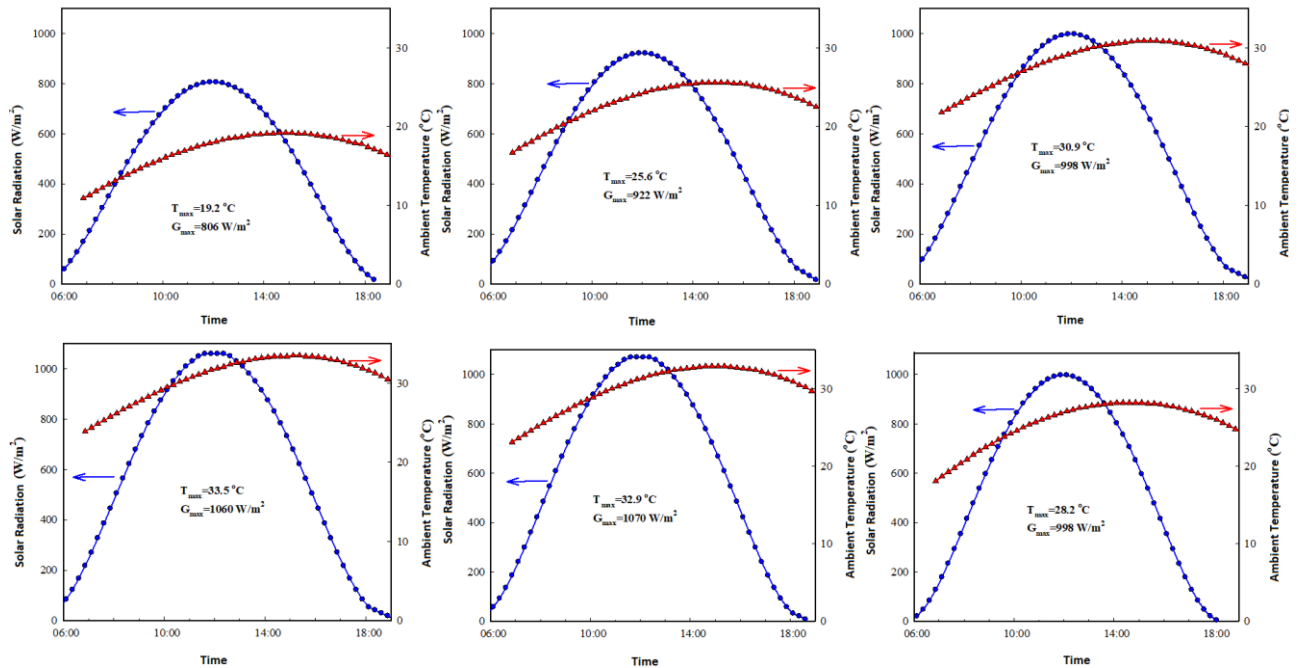
Fig. 9. Average temperature and radiations for the test period

September. The highest maximum average radiation value was obtained in August and the lowest maximum average radiation value was obtained in April.

Similarly, ambient temperature values were measured every 15 minutes during the daytime and monthly average values were calculated. Average ambient temperatures and average solar radiations for April and September are presented in Fig 9. Monthly average ambient temperature was 19.2 °C for April, 25.6 °C for May, 30.9 °C for June, 33.5 °C for July, 32.9°C for August, and 28.2 °C for September. The highest temperature was measured as 38.2 °C at 14:55 on July 23
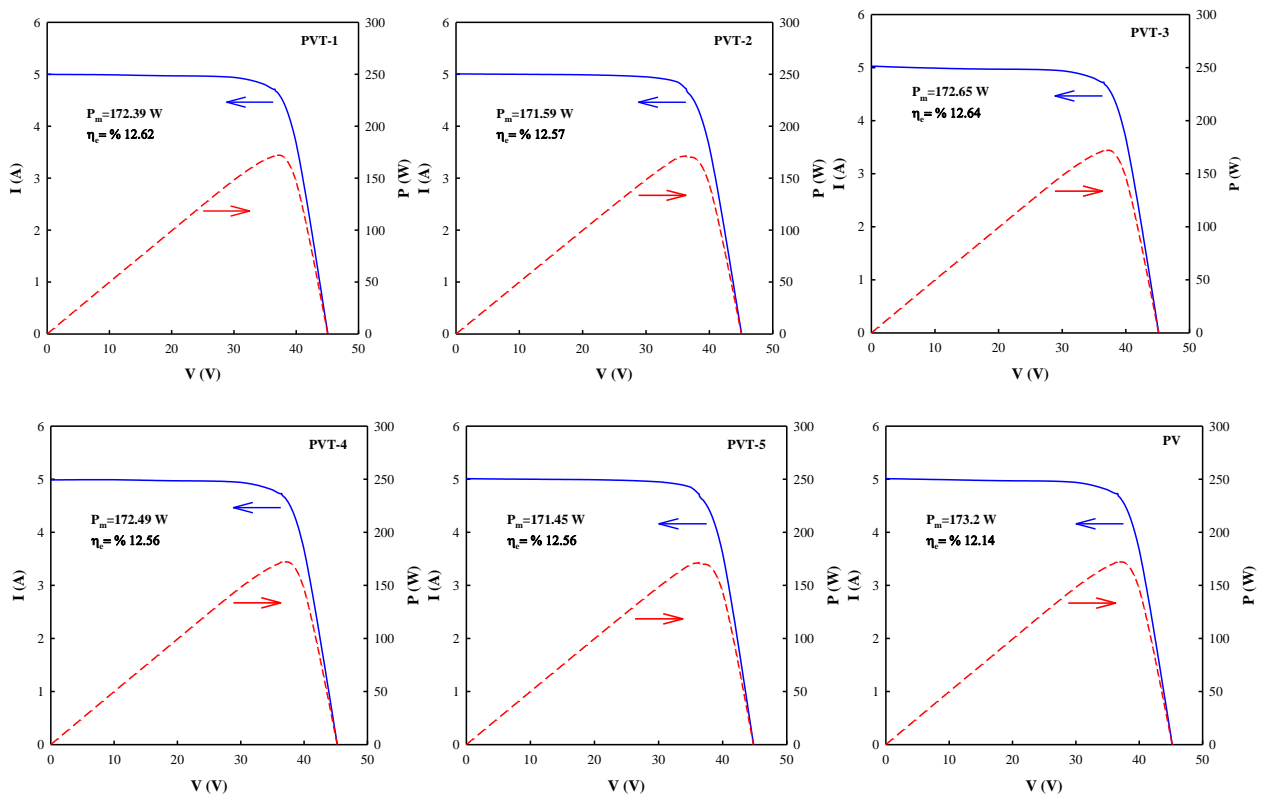
Fig. 10. I-V-P curve of the PV/T-1, 2, 3, 4, 5 and PV module.

Current-Voltage (I-V) values of the fabricated modules (PV/T and PV) under standard test conditions (STC) were measured. The measurement results of the PVT modules are presented in Fig 10. In addition, the fill factor and the efficiency value of each module was calculated using and presented in Table 3. It can be inferred that the power values of the modules vary between 171.45 W and 173.19 W, while their electrical efficiency values are between 12.57% and 12.68%. Although identical PV cells were used in all modules and same number of PV cells in each module, slight differences were observed in electrical parameters and efficiency values. This could be attributed to the minimal changes in cell efficiency.

current values of the PVT-5 module are greater than those of other modules whereas the PVT-3 module yielded the lowest current values. As known, the current values of PV cells slightly increase with increasing temperature. However, this causes a significant decrease in the voltage. Therefore, this results in a decrease in the performance, i.e., efficiency, of the PV cells. When compared to the other modules, the thermal part of the PVT-3 module provides more efficient cooling in terms of cell temperature values, enabling cells in this module to convert energy at lower cell temperatures. The order of current values of all PV/T modules from low to high is as follows: PVT-3<PVT-4<PVT-1<PVT-2<PVT-5.

In addition, because the ambient temperature is low

Table 3. Electrical parameters and efficiency values of the samples under STC

Sample Name	V_{oc} (V)	V_m (V)	I_{sc} (A)	I_m (A)	P_m (W)	FF	η_e (%)
PVT-1	45.22	36.57	4.998	4.714	172.39	0.763	12.62
PVT-2	45.08	36.34	5.007	4.722	171.59	0.760	12.57
PVT-3	45.17	36.54	5.027	4.725	172.65	0.760	12.64
PVT-4	45.25	36.46	4.986	4.731	172.49	0.765	12.63
PVT-5	44.82	36.31	5.010	4.722	171.45	0.764	12.56
PV	45.21	36.60	5.011	4.732	173.19	0.763	12.68

Fig 11 demonstrates the daily radiation and electrical current changes of the PVT-1, PVT-2, PVT-3, PVT-4, PVT-5, and the PV modules, respectively. The measurements showed that the increase in solar radiation values slightly increased the current values of the PV/T and PV modules. Also, when the change in current values of each PV/T module is examined, it can be seen that the

under low radiation conditions and therefore cell temperature values are very close to each other, there was no difference in the current values of the PV/T modules and the PV module. However, since the cells in the PV/T modules are cooled by the thermal part during the time with high radiation values, the PV/T modules have lower current values than the PV module. Since there is no
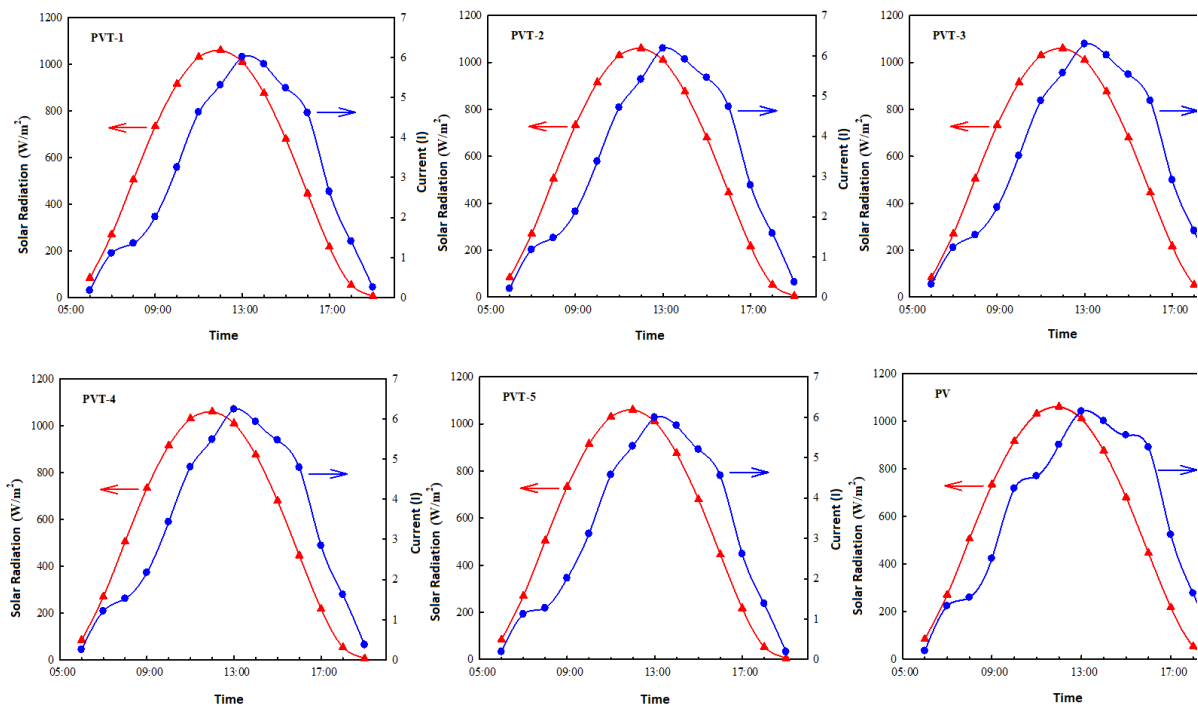
Fig. 11. Daily radiation and electrical current change of the PV/T and PV modules

cooling in the PV module, the cells become more heated and higher current values are obtained.

The electrical power values of the PV/T modules and the PV module were also determined by current-voltage measurements. Fig 12 demonstrates the daily average electrical power values of the PVT and PV modules. During the day, at 13:00 and under 1010 W/m^2 radiation, 35°C ambient temperature, and 0.83 m/s wind speed, the PVT-3 module yielded 7.37 W of electrical power, more

values under ambient conditions were measured as 11.5%, 11.4%, 12.4%, 11.8%, 11.1%, and 9.9% for the PVT-1, PVT-2, PVT-3, PVT-4, PVT-5, and PV modules, respectively. Besides, maximum efficiency values during the day were measured as 12.9%, 12.6%, 13.2%, 13.0%, 12.0%, and 10.5% for the PVT-1, PVT-2, PVT-3, PVT-4, PVT-5, and PV modules, respectively. It is revealed that PV/T 3 yielded the maximum electrical efficiencies.
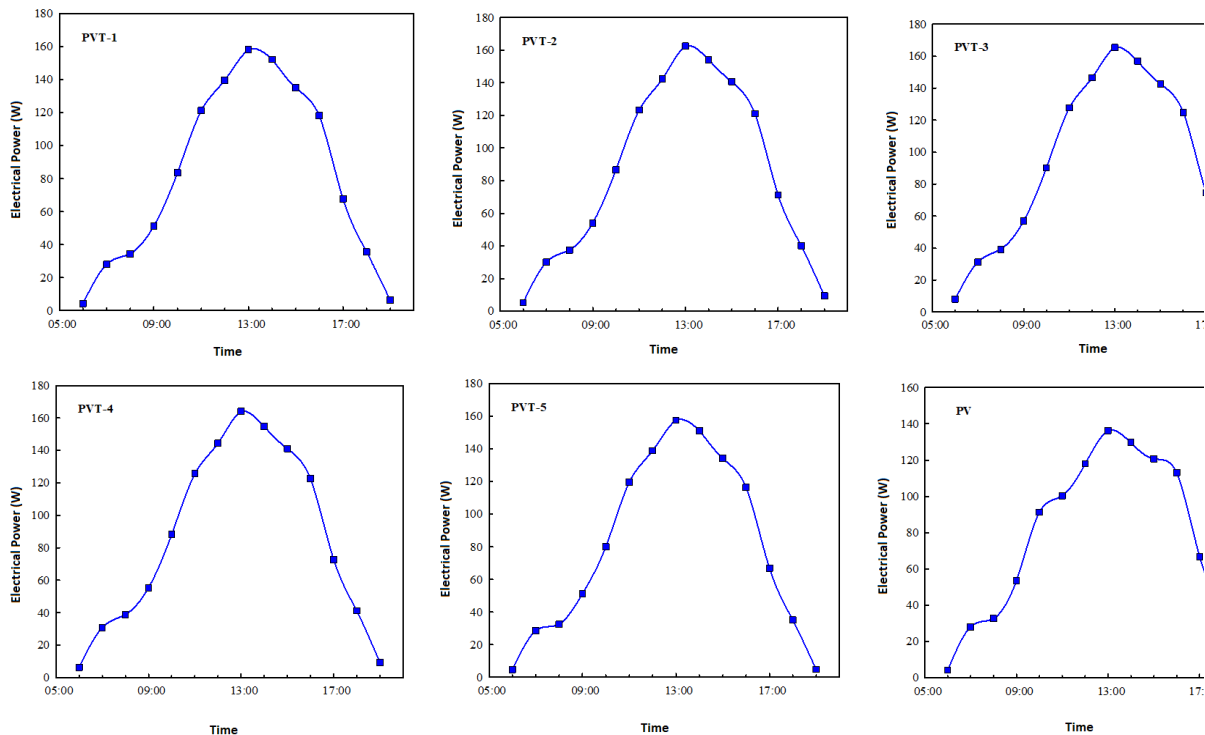
Fig. 12. Daily average electrical power values of the PVT module for July.

than PVT-1, PVT-2, PVT-4, PVT-5, and PV modules as 2.9 W, 1.32 W, 7.89 W, and 29.29 W, respectively. The average daily total electrical energy produced was measured as 1135.28 Wh, 1178.28 Wh, 1216.70 Wh, 1195.31 Wh, 1121.39 Wh, and 1035.77 Wh for the PVT-1, PVT-2, PVT-3, PVT-4, PVT-5, and PV modules, respectively. Accordingly, the PVT-3 module yielded the highest energy conversion.

Variations of the electrical efficiency of each module by cell temperature under 1000-1060 W/m^2 radiation, 35-36 °C ambient temperature, and 0.8-0.85 m/s wind speed are presented in Fig 13 for the PVT and PV modules, respectively. Average electrical conversion efficiency

To investigate the cell cooling performance of the modules with different absorber structures, temperature sensors were placed on the PV/T modules in contact with the PV cells and surface temperatures were measured. The average values of the measurements performed in July, highest temperature and radiation values attained, are presented in

Fig 14. Detailed examination of the values of the PV/T modules having different structures in terms of thermal part showed that the PVT-3 module has the highest surface cooling value. Similarly, the maximum surface temperature averages measured for each module are presented in Table 4.
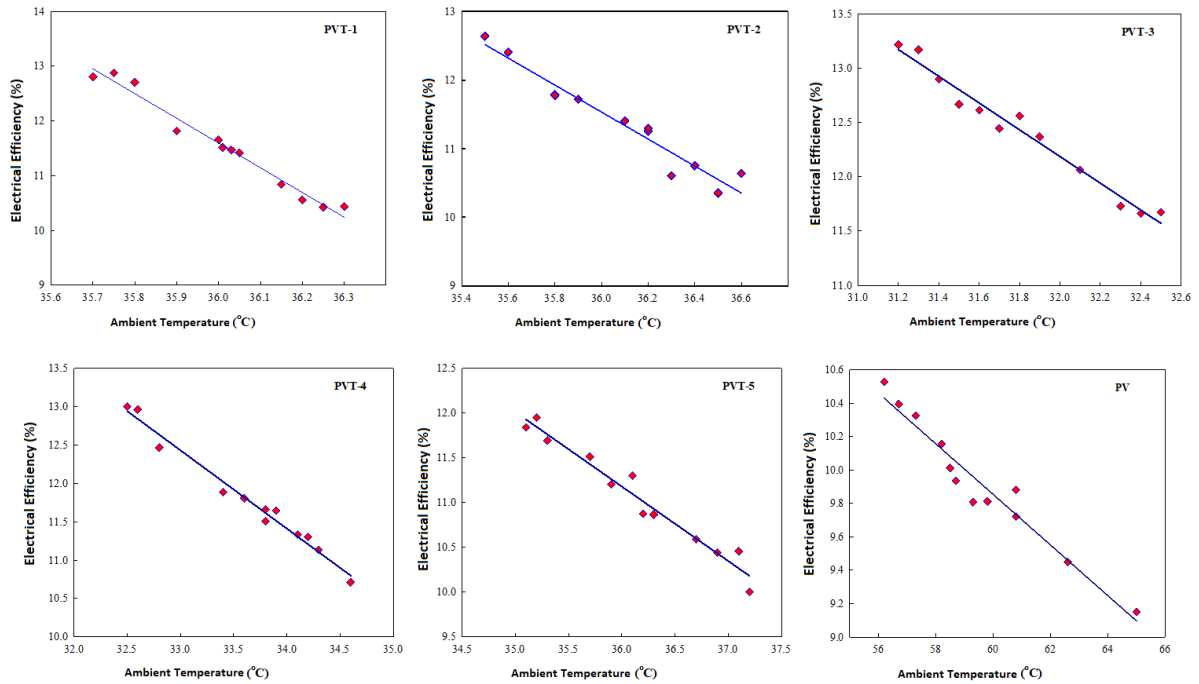
Fig. 13. Variation of the electrical efficiency of the PV/T and PV modules by cell temperature.
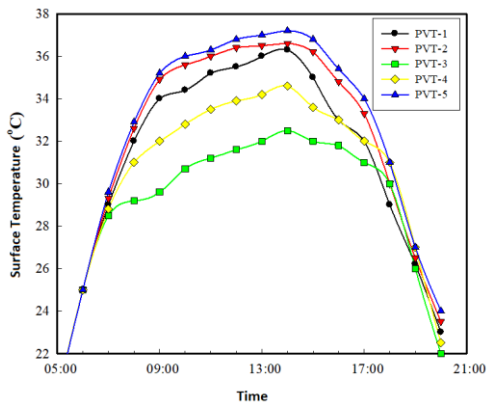
Fig. 14. Average surface temperatures of the PV/T modules for July

Table 4 Maximum surface temperature of modules

Sample	Maximum Surface Temperature (°C)
PVT-1	36.3
PVT-2	36.6
PVT-3	32.5
PVT-4	34.6
PVT-5	37.2
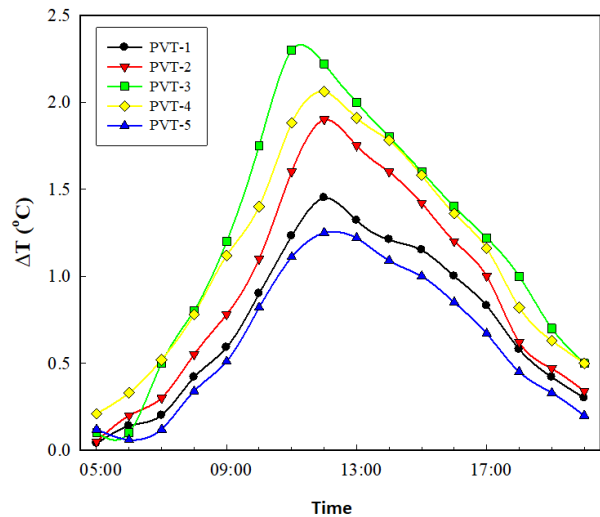
Fig 15. Variation of water input-output temperature differences of the PV/T modules

In order to calculate the thermal gain and thermal efficiency values of PV/T modules, the water input and output temperatures must be obtained. Variation of water inlet-outlet temperature differences of the modules under 806 W/m^2 solar radiation, 28.6 °C ambient temperature, and 0.045 kg/s input flow rate are presented in Fig 15. Values were taken as the difference in water temperatures in the boiler of each system. Temperature differences were calculated as 1.45 °C, 1.9 °C, 2.3 °C, 2.06 °C, and 1.25 °C for the PVT-1, PVT-2, PVT-3, PVT-4, and PVT-5 modules, respectively.

Also, water input-output temperature values of the PV/T modules under 1050 W/m^2 radiation, 32.5°C ambient temperature, and 0.045 kg/s input flow rate are presented in Table 5. In these experiments, module input temperatures were kept constant at 33°C (above ambient temperature) and the temperature difference values of each collector were examined. The experiments were performed to calculate the temperature differences and efficiency values of each module at the highest radiation and temperature conditions of the day. When the results were examined, the highest thermal efficiency was obtained from the PVT-3 module.

temperature difference in the PVT-5 module, followed by PVT-3, PVT-1, PVT-2, and PVT-4 modules

Using the results of the measurements performed at one-hour intervals in a day throughout July, thermal efficiency values were calculated for each PV/T module and monthly averages for each measurement time were determined. Average thermal efficiency variations of the PVT modules in July are presented in Fig 17. Maximum thermal efficiency values in a day were calculated as 50.1% for the PVT-1, 51.3% for the PVT-2, 54.3% for the PVT-3, 51.8% for the PVT-4, and 49.2% for the PVT-

Sample	T_o (°C)	Wind Speed (m/s)	Radiation (W/m)^2)	T_g (°C)	$T_ç$ (°C)	Mass Flow (kg/h)	ΔT (°C)
PVT-1	32.5	1	1050	33	36.78	0.045	3.78
PVT-2	32.5	1	1050	33	36.86	0.045	3.86
PVT-3	32.5	1	1050	33	37.10	0.045	4.10
PVT-4	32.5	1	1050	33	36.90	0.045	3.90
PVT-5	32.5	1	1050	33	36.70	0.045	3.70

Table 5. Water inlet-outlet temperature values of the PV/T modules

Based on the measurement results given in Table 5, the thermal efficiencies of PV/T modules were calculated and the corresponding results are presented in Table 6. When the results were examined, the highest thermal efficiency was obtained from the PVT-3 module.

5 module. PV/T-3 retains the highest thermal efficiency as compared to others.

As can be seen from the figures, since the radiation values were low in the early morning and evening hours, the efficiency values were modest, however, since the

Table 6. Thermal parameters and efficiencies of the PV/T modules under the same conditions

	Sample	PV/T-1	PV/T-2	PV/T-3	PV/T-4	PV/T-5
Ambient conditions	T_o (°C)	32.5	32.5	32.5	32.5	32.5
	Wind speed (m/s)	1	1	1	1	1
	Radiation	1050	1050	1050	1050	1050
PV/T module	Aperture area (m^2)	1.365	1.365	1.365	1.365	1.365
	Absorber area (m^2)	1.36	1.36	1.36	1.36	1.36
PV/T module measurement	T_g (°C)	33	33	33	33	33
	T_c (°C)	36.78	36.86	37.1	36.9	36.7
	Mass flow (kg/h)	0.045	0.045	0.045	0.045	0.045
Calculations	ΔT (°C)	3.78	3.86	4.10	3.90	3.70
	T_m (°C)	34.89	34.93	35.05	34.95	34.85
	C_p (Ws/kg°C)	4175	4175	4175	4175	4175
	T_m-T_o (°C)	2.39	2.43	2.55	2.45	2.35
	Reduced Temperature Difference	0.0022	0.0023	0.0024	0.0023	0.0022
	Useful Power (W)	710	725	770	733	695
	Instantaneous Efficiency (Aperture area)	0.495	0.506	0.537	0.511	0.485
	Instantaneous Efficiency (Absorber area)	0.497	0.508	0.539	0.513	0.487

During the test campaign, solar radiation dependent temperature differences of water inlet and outlet were measured as well. The differences in water input-output temperatures are presented in Fig 16. It is shown that the decrease in radiation has the most effecting factor on the

radiation values between 08:00 and 18:00 are more stable, the efficiency values were more realistic. At noon, on the other hand, the thermal efficiency was at maximum plateau due to the radiation being at the highest value of the day. In the literature, usually, results related to thermal efficiencies of systems are provided

while losses due to temperature are not taken into account.

Chow et al. [25] and Tripanagnostopoulos et al. [26] found the thermal efficiencies of the PV/T modules they investigated between 38% and 48%. In this study, on the other hand, the thermal efficiencies were attained ranging from 49% to 56% depending on the flow rate. This result, which is consistent with the literature, shows that laminating photovoltaic cells with an absorber plate increases the efficiency.

The thermal and electrical efficiencies of all PV/T modules are presented in Fig 18a and the maximum total efficiency values are presented in Fig 18b as well. As can be seen from Figure 18a, the maximum electrical efficiency values are between 12% and 13.2%. In addition, the maximum thermal efficiency values, which are higher than the electrical efficiency values, are between 48% and 54% as shown in Fig 18b. It is shown that the thermal efficiency values deviated more than the electrical efficiencies. The reason for this fluctuation is
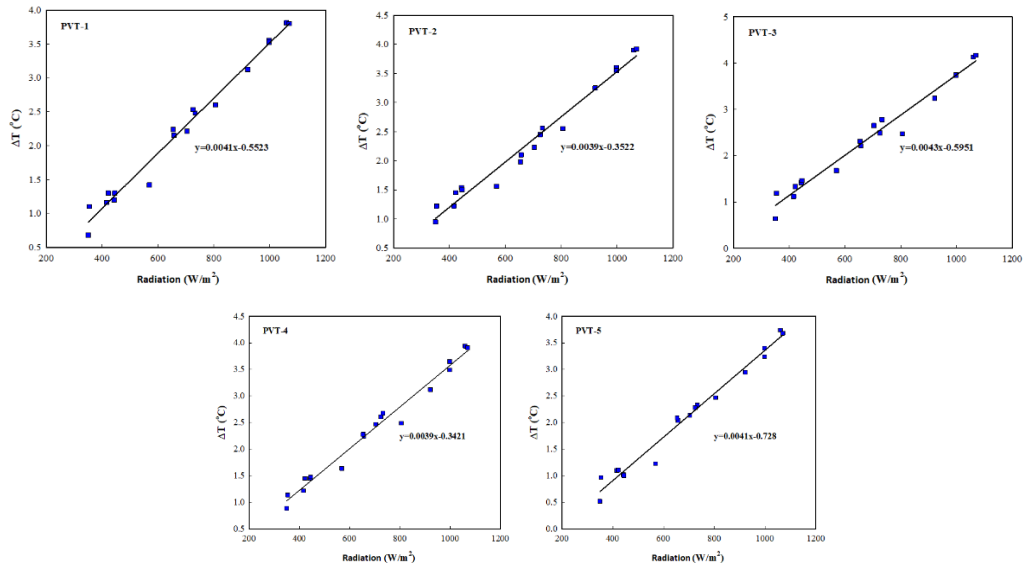
Fig 16. Variation of water input-output temperature differences of the PVT-5 module by radiation
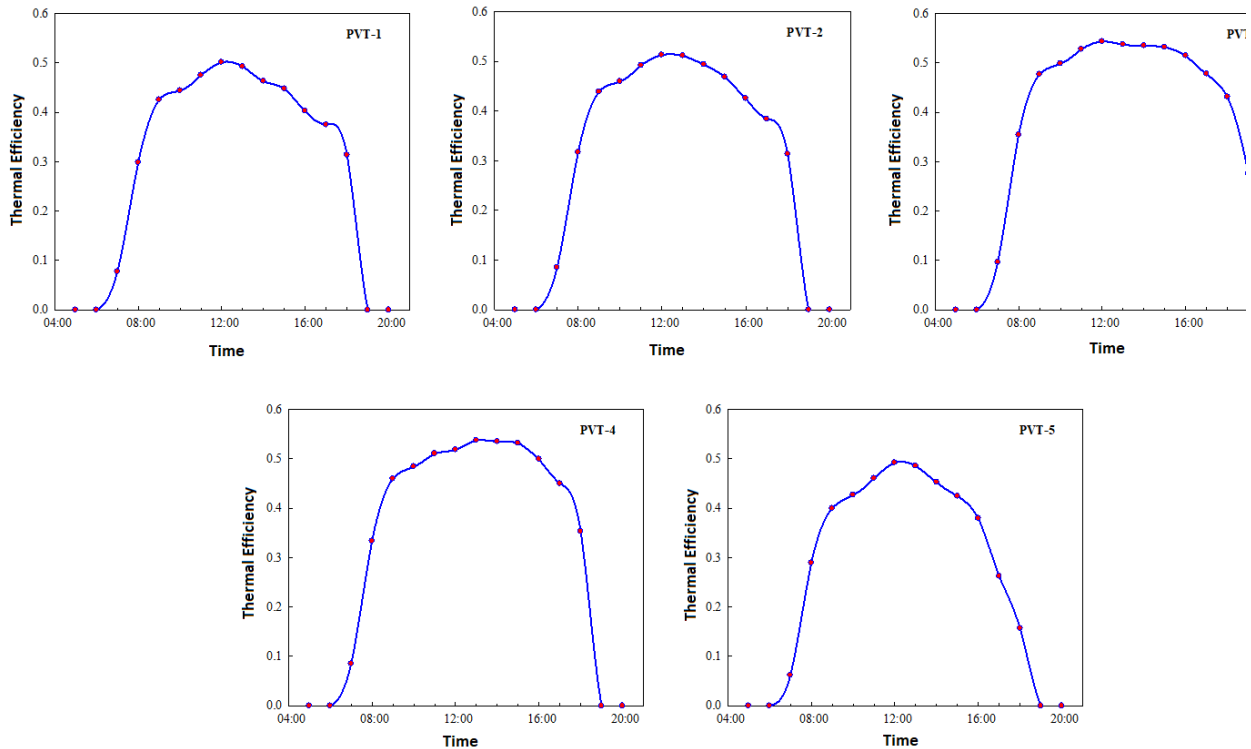
Fig 17. Average thermal efficiency variation of the PVT-5 module for July.

that the thermal efficiency does not change depending only on radiation but also on ambient temperature, heat loss, and other meteorological parameters. Depending on these factors, the thermal efficiency of a PV/T system varies. When compared in terms of total efficiency, the PVT-1 module yielded a maximum efficiency of 62.63%, the PVT-2 module with 63.38%, the PVT-3 module with 67.14%, the PVT-4 module with 64.31%, and the PVT-5 with module 60.68%, respectively. As can be seen from these results, the efficiency of the PVT-3 module was higher than other PV/T modules.

configurations has been carried out under prevailing weather conditions of Izmir. The PV/T and PV modules were installed in the south-face roof of the Ege University's Institute of Solar Energy building and monitored between April and December 2012. The main aim of the this study is to investigate the PV/T modules produced with modified absorbers of different diameters and types under the same conditions to find out the optimum PV/T module in terms of both electrical and thermal performance. For the electrical performance, fabricated PV/T units and a PV module were tested under
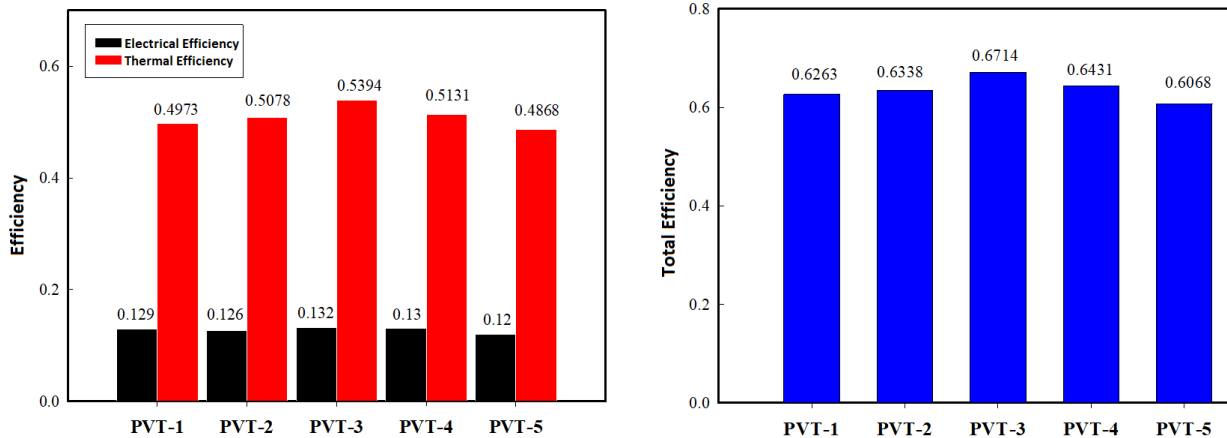
Fig 18. Maximum a) electrical and thermal and b) total maximum efficiencies of the PV/T modules

The instantaneous maximum electrical and thermal power values of the PV/T modules are presented in Fig 19a and the total (combined electrical and thermal) maximum power values are presented in Fig 19b. Maximum thermal energy conversion values vary between 703 W and 783 W while electrical energy conversion values vary between 153 W and 168 W. In addition, total maximum power values are ranging from 856 W and 951 W and maximum conversion is obtained from PVT-3 module.

the same ambient conditions and performance outcomes were compared to detect the cooling effect of the water circulation through the absorbers on the electrical efficiencies. For the thermal performance, similarly, PV/T modules were examined under the same test conditions and thermal performances were observed. Based on the results and findings, concluding remarks can be drawn as follows;

The power rates of the modules obtained varied between
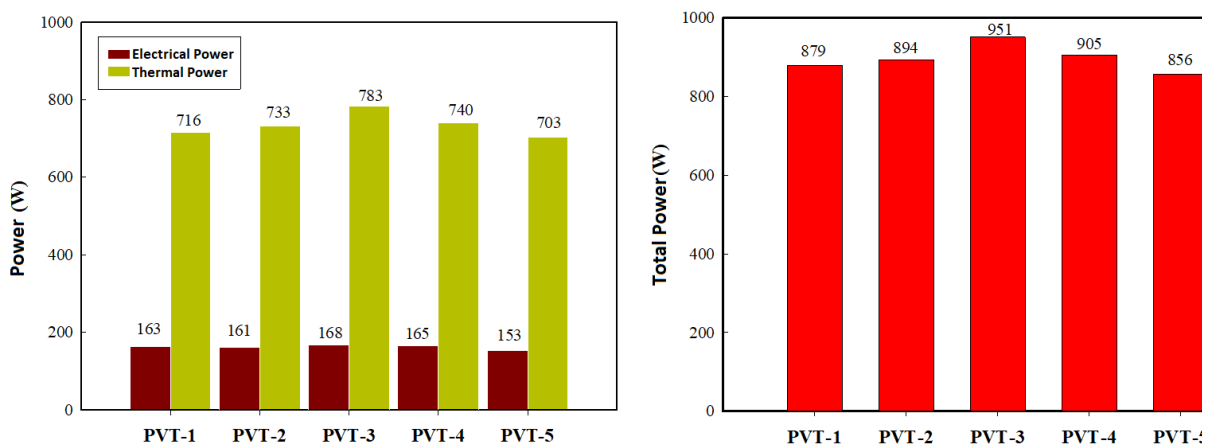
Fig 19. Maximum a) electrical and thermal power and b) total maximum power values of the PV/T modules

5. CONCLUSION

In this study, experimental investigation on the performance parameters that affect the efficiency of water type PV/T collectors with modified absorber

171.45 W and 173.19 W, while their electrical efficiencies were between 12.57% and 12.68%. As is known, the current values of PV cells increase, albeit slightly, with increasing temperature. However, despite

this small increase in current with the increasing temperature, there is a significant decrease in the voltage value. This results in a decrease in the performance, i.e., efficiency, of the PV cells.

The cells in the PV/T modules were cooled by the thermal part during the time with high radiation values, the PV/T modules had lower current values than the PV module. Since the PV module was not cooled, the cells encapsulated more heat and corresponding electrical efficiency was relatively lower.

Compared to the other modules, the thermal part of the PVT-3 module provides more efficient cooling in terms of cell temperature values, enabling cells in this module to convert energy at lower cell temperatures. When the results were examined, the highest thermal efficiency was obtained from the PVT-3 module. Similarly, the PVT-3 module yielded the highest actual useful power of 783 W. The total maximum efficiency of the PVT-3 is also the highest with 67%. Therefore, PVT-3 is the optimum module among others studied.

Abbreviations

G	Global Radiation	E_{Fp}	Fermi Energy for the p-type semiconductor	η_e	Electrical Efficiency
G_{sc}	Solar Constant	eV	Electron Volt	k	Boltzmann Constant
D	Diffuse Radiation	I	Current	P_{in}	Radiation on Cell or Module
B	Direct Radiation	V	Voltage	R_s	Series Resistance
ρ	Albedo	n	Ideality Factor	R_p	Parallel Resistance
Z	Zenit Angle	I_L	Current under radiation	V_R	Reverse Supply Voltage
ϕ	Latitude Angle	I_s	Saturation Current	V_{bi}	Internal Potential Barrier in Thermal Balance
ω	Clock Angle	I_{sc}	Short Circuit Current	$\vec{E}$	Internal Electric Field
δ	Inclination Angle	V_{oc}	Open Circuit Voltage	W	Width of the Depletion Layer
AMm	Air mass	I_m	Maximum Current	$\alpha\,(v)$	Absorption Coefficient
E_v	Upper Energy Level of Valence Band	V_m	Maximum Voltage	L_D	Diffusion Length
E_c	Lower Energy Level of Conductivity Band	P_m	Maximum Power Point	N	Number of Series-Connected PV Cells
E_g	Forbidden Energy Range	FF	Fill Factor	V_T	Thermal Voltage
E_F	Fermi Energy	e	Electron Charge	η_{ref}	Efficiency of the PV Module under STC
E_{Fn}	Fermi Energy for the n-type semiconductor	K	Kelvin	$\mu_{P,mp}$	Module Efficiency Temperature Coefficient
A_t	Collector Surface Area	T_i	Fluid Input Temperature	T_o	Fluid Output Temperature
$\dot{m}$	Mass Flow	c_p	Specific Heat	η_t	Thermal Efficiency
K	Heat Loss Coefficient	K_{low}	Lower Surface Heat Loss Coefficient	K_{top}	Top Surface Heat Loss Coefficient
S	Absorbed Solar Energy	U_L	*Collector Heat Loss Coefficient*	$T_{p,m}$	*Average Temperature of an Absorber Plate*
C_b	Conductivity between an absorber plate and pipe	F	Absorber Plate Efficiency Factor	D_i	Fluid Pipe Diameter
w	Distance	η_T	Total Efficiency	ΔT	Input- Output Water Temperature Differences
ΔT^*	Water Input-Ambient Temperature Differences	GS	Day Time	V_f	Direct Supply Voltage
V_r	Reverse Supply Voltage	TS	Woven Patterned Surfaces	EVA	Ethyl Vinyl Acetate
TPT	Tedlar Polyester Tedlar	$NOCT$	Nominal Working Cell Temperature	STC	Standard Test Conditions
CEC	Cooling Effect Coefficient				

PV/T systems jointly produce electrical and thermal power and offer high efficiencies both end. As active cooling of the PV cells results in enhanced electrical efficiencies while swept heat is accumulated by means of thermal storage which can be used in variety of applications including heating, ventilation and air conditioning. Therefore, widespread utilization of these technologies is of great importance towards energy efficiency and sustainability.

ACKNOWLEDGEMENT

DECLARATION OF ETHICAL STANDARDS

The authors of this article declare that the materials and methods used in this study do not require ethical committee permission and/or legal-special permission.

AUTHORS' CONTRIBUTIONS

Halil Ibrahim DAG: Performed the experiments and analyse the results, writing—original draft preparation.

Günnur KOCAR: Conceptualization, supervision, writing—review and editing.

CONFLICT OF INTEREST

There is no conflict of interest in this study

REFERENCES

[1] Dag, H. I.; Buker, M. S., "Performance evaluation and degradation assessment of crystalline silicon based photovoltaic rooftop technologies under outdoor conditions", *Renewable Energy*, (2019).

[2] Buker, M. S.; Riffat, S. B., "Preliminary performance test of a combined solar thermal roof system with heat pump for buildings", *Energy Procedia*, 91: 421-431, (2016).

[3] Perlin, J., "Let it shine: the 6,000-year story of solar energy", *New World Library*, (2013).

[4] *www.iea.org*, "Solar PV report", (2019).

[5] Buker, M. S.; Riffat, S. B., "Performance analysis of a combined Building Integrated PV/T Collector with a liquid desiccant enhanced dew point cooler", *Energy Procedia*, 91: 717-727, (2016).

[6] Böer, K. W.; Tamm, G., "Solar conversion under consideration of energy and entropy", *Solar Energy*, 74(6): 525-528, (2003).

[7] Zondag, H. A. "Flat-plate PV-Thermal collectors and systems: A review", *Renewable and Sustainable Energy Reviews*, 12(4): 891-959, (2008).

[8] Kalogirou, S. A.; Tripanagnostopoulos, Y., "Hybrid PV/T solar systems for domestic hot water and electricity production", *Energy conversion and management*, 47(18-19): 3368-3382, (2006).

[9] Koç, İ.; Başaran, K., "PV/T Tabanlı Bir Sistemde MATLAB/Simulink Kullanılarak Yapılan Performans Analizi", *Politeknik Dergisi*, 22(1): 229-236.

[10] Kumar, R.; Rosen, M. A., "Performance evaluation of a double pass PV/T solar air heater with and without fins", *Applied Thermal Engineering*, 31(8-9): 1402-1410, (2011).

[11] Al-Waeli, A. H., Sopian, K., Kazem, H. A., Yousif, J. H., Chaichan, M. T., Ibrahim, A., ... & Ruslan, M. H., "Comparison of prediction methods of PV/T nanofluid and nano-PCM system using a measured dataset and artificial neural network", *Solar Energy*, 162: 378-396, (2018).

[12] Rejeb, O.; Dhaou, H.,; Jemni, A., "A numerical investigation of a photovoltaic thermal (PV/T) collector", *Renewable Energy*, 77: 43-50, (2015).

[13] Liang, R., Zhang, J., Ma, L., & Li, Y., "Performance evaluation of new type hybrid photovoltaic/thermal solar collector by experimental study", *Applied Thermal Engineering*, 75: 487-492, (2015).

[14] Aste, N.; Leonforte, F.; Del pero, C., "Design, modeling and performance monitoring of a photovoltaic–thermal (PVT) water collector", *Solar Energy*, 112: 85-99, (2015).

[15] Neamen, D. A., "Semiconductor physics and devices: basic principles", *New York, NY: McGraw-Hill,*, (2012).

[16] Möller, H. J., "Semiconductors for solar cells", *Artech House Publishers*, (1993).

[17] Duffie, J. A.; Beckman, W. A., "Solar engineering of thermal processes", *New York: Wiley*, (1991).

[18] Radziemska, E., "Thermal performance of Si and GaAs based solar cells and modules: a review", *Progress in Energy and Combustion Science*, 29(5): 407-424, (2003).

[19] Buker, M. S.; Riffat, S. B., "Building integrated solar thermal collectors–A review", *Renewable and Sustainable Energy Reviews*, 51: 327-346, (2015).

[20] Zondag, H. A., "Flat-plate PV-Thermal collectors and systems: A review", *Renewable and Sustainable Energy Reviews*, 12(4): 891-959, (2008).

[21] Charalambous, P. G., Kalogirou, S. A., Maidment, G. G., & Yiakoumetti, K. (2011), "Optimization of the photovoltaic thermal (PV/T) collector absorber", *Solar energy*, 85(5): 871-880, (2011).

[22] Hottel, H., & Whillier, A., "Evaluation of flat-plate solar collector performance", *In Trans. Conf. Use of Solar Energy 3:* (1955).

[23] He, W., Chow, T. T., Ji, J., Lu, J., Pei, G., & Chan, L. S., "Hybrid photovoltaic and thermal solar-collector designed for natural circulation of water", *Applied energy*, 83(3): 199-210, (2006).

[24] Vokas, G.; Christandonis, N.; Skittides, F. "Hybrid photovoltaic–thermal systems for domestic heating and cooling—a theoretical approach", *Solar Energy*, 80(5): 607-615, (2006).

[25] Chow, T. T.; HE, W.; JI, J. "An experimental study of facade-integrated photovoltaic/water-heating system", *Applied thermal engineering*, 27(1): 37-45, (2007).

[26] Tripanagnostopoulos, Y., Souliotis, M., Battisti, R., & Corrado, A., "Energy, cost and LCA results of PV and hybrid PV/T solar systems", *Progress in Photovoltaics: Research and applications*, 13(3): 235-250, (2005).

[27] Dağ, H. İ. "Pv-termal kolektörlerin tasarımı, üretimi ve verimini etkileyen parametrelerin belirlenmesi", *PhD Thesis. Doktora Tezi, Ege Üniversitesi, Fen Bilimleri Enstitüsü, İzmir*, (2015).